

Structural Connection Parameter Measurement for Precision Motion Systems Using Accelerometers: A Preliminary Study

Li Li¹, Zheng Yang¹, Jia Ziqing¹

¹ Center of Ultra-precision Optoelectronic Instrument Engineering, Harbin Institute of Technology, Harbin, China, hitlili@hit.edu.cn, 24s001063@stu.hit.edu.cn, 120L011718@stu.hit.edu.cn

Abstract – Accurate modelling is important for both the performance control and monitoring of high-precision motion systems in advanced manufacturing machines. It is not difficult to build dynamic models for motion systems based on the multi-rigid-body system assumption. However, it is usually not feasible to acquire the real connection parameters between rigid bodies like stiffness and damping coefficients especially after mechanical assembly which can be significantly different from their designed values. In this paper, a measurement scheme using multiple accelerometers is presented with discussion of the data processing methods. Simulation results on a three-rigid-body motion system and experimental results on a two-mass motion system preliminarily verify the scheme. Finally, existing problems are put forward for further study.

I. INTRODUCTION

High precision motion systems are indispensable parts in advanced manufacturing machines, which play important roles in improving the machine accuracy and productivity [1-2]. Modeling is the primary step for the performance control and monitoring during the life-cycle of the motion system [3-4]. In practice, the high-precision motion systems can usually be described as multi-rigid-body systems [5]. A typical example is the lithography machine used for wafer scanning, in which the wafer stage can be simplified as an open-loop chain lumped mass-spring-damper model as shown Fig.1 [6]. Based on this assumption, it is not difficult to derive the mathematical dynamic model which can be used for performance evaluation [7]. However, despite the derived model structure can grasp the major features of the system dynamics, the accuracy of the model parameters will affect the authenticity of the evaluation results [8]. Since the mass values of mechanical parts can be known exactly before assembly, the structural connection parameters such as the stiffness and damping coefficients are the unknown model parameters which are required to be determined [9]. These parameters can only be determined after assembly, and their real values are usually significantly different

from the design values.

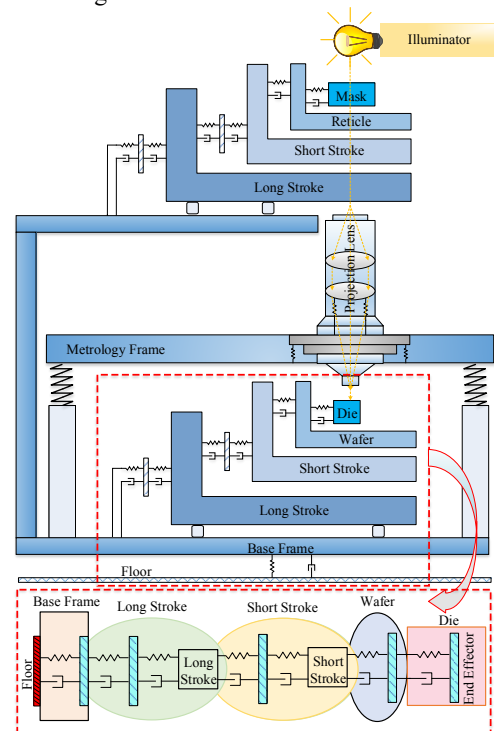


Fig.1 Schematic diagram of lithography machine and open-loop chain lumped mass-spring-damper model of wafer stage [6].

In this paper, the modeling of one translational DOF (degree of freedom) of the multi-rigid-body motion system is considered as an illustrated example. Based on the multi-rigid-body model structure and the already known mass values of the mechanical parts, multiple accelerometers are utilized to measure the structural connection parameters. The measurement scheme is presented and the data processing methods are discussed. Simulation results can verify the above theoretical results. In addition, the first version of the wireless measurement device is developed and preliminary experimental results are obtained. Finally, existing problems are discussed which are required to be solved in the future study.

II. MEASUREMENT SCHEME

Without loss of generality, the n -rigid-body system is considered here and can be shown in Fig.2. Denote x_i as the output (displacement [m]) of the i th rigid body. Denote m_i , k_i and b_i as the mass, stiffness and damping coefficients. Then it can be derived that

$$\sum_{j=i}^n m_j \ddot{x}_j = b_i(\dot{x}_{i-1} - \dot{x}_i) + k_i(x_{i-1} - x_i) \quad (1)$$

For the n -rigid-body system, n equations like Eq.(1) can be built, which are summarized as follows:

$$\begin{cases} m_n \ddot{x}_n = b_n(\dot{x}_{n-1} - \dot{x}_n) + k_n(x_{n-1} - x_n) \\ \vdots \\ \sum_{j=i}^n m_j \ddot{x}_j = b_i(\dot{x}_{i-1} - \dot{x}_i) + k_i(x_{i-1} - x_i) \\ \vdots \\ \sum_{j=2}^n m_j \ddot{x}_j = b_2(\dot{x}_1 - \dot{x}_2) + k_2(x_1 - x_2) \\ \sum_{j=1}^n m_j \ddot{x}_j = -b_1 \dot{x}_1 - k_1 x_1 \end{cases} \quad (2)$$

It should be noted that the known control input signals

are neglected in above equations for the simplicity of the presentation, which will be considered and discussed in the future study.

Denote \ddot{x}_i as a_i , $i = 1, \dots, n$ which can be obtained by using accelerometers. The measurement value is denoted as \tilde{a}_i , which is corrupted with the measurement noises v_i . It means that $\tilde{a}_i = a_i + v_i$.

Then, the measurement scheme using wireless accelerometers to obtain the structural connection parameters for the multi-rigid-body motion system can be shown in Fig.2. It is clear that the data processing method will be the core of the scheme, the aim of which is to obtain the estimated values of b_i and k_i , denoting as \hat{b}_i and \hat{k}_i , if m_i, m_{i+1}, \dots, m_n are supposed to be known values.

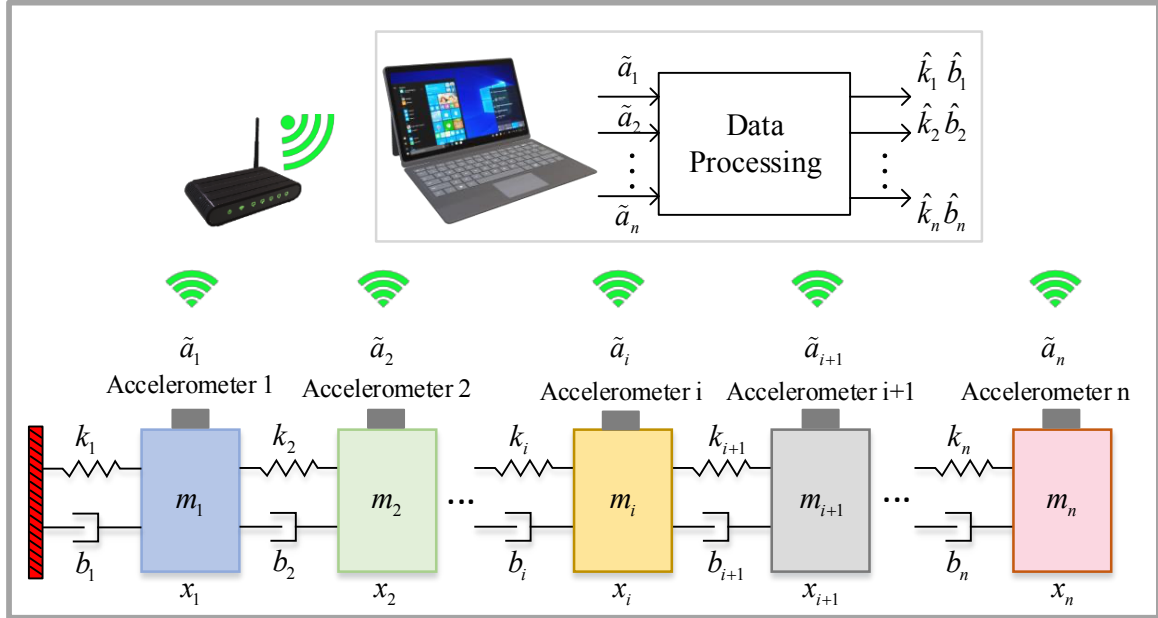


Fig.2 Schematic diagram of n -rigid-body system and its structural connection parameter measurement scheme.

III. DATA PROCESSING METHOD

In this section, the following two candidate methods that can be used for data processing are discussed:

A. Least-square method

Transform Eq.(1) into the following linear regression equation

$$y_i = \boldsymbol{\varphi}_i \boldsymbol{\theta}_i \quad (3)$$

where

$$y_i = \sum_{j=i}^n m_j a_j$$

$$\boldsymbol{\varphi}_i = [\int a_{i-1} - \int a_i \quad \int \int a_{i-1} - \int \int a_i]$$

$$\boldsymbol{\theta}_i = \begin{bmatrix} b_i \\ k_i \end{bmatrix}$$

Define the following vectors and matrices

$$\mathbf{Y}_i = [y_i(t_1) \quad \dots \quad y_i(t_N)]^T$$

$$\boldsymbol{\Phi}_i = [\boldsymbol{\varphi}_i^T(t_1) \quad \dots \quad \boldsymbol{\varphi}_i^T(t_N)]^T$$

where $y_i(t_1), \dots, y_i(t_N)$ represent the N sample values of the signal y_i at time instants t_1, \dots, t_N , where $t_i = (i-1)T_s$, T_s is sampling period, $i = 1, \dots, N$.

Then, Eq.(3) can be transformed into that

$$\mathbf{Y}_i = \boldsymbol{\Phi}_i \boldsymbol{\theta}_i \quad (4)$$

Using the least-square method, it can be obtained that

$$\hat{\boldsymbol{\theta}}_i = (\boldsymbol{\Phi}_i^T \boldsymbol{\Phi}_i)^{-1} \boldsymbol{\Phi}_i^T \mathbf{Y}_i$$

Considering the noise effect, the following equation can provide the estimate of $\boldsymbol{\theta}_i$:

$$\hat{\theta}_i = (\tilde{\Phi}_i^T \tilde{\Phi}_i)^{-1} \tilde{\Phi}_i^T \tilde{Y}_i \quad (5)$$

where $\tilde{\Phi}_i$ and \tilde{Y}_i are constructed with the measurement values of the accelerometers.

B. Frequency-domain identification method

Transform Eq.(1) into the following equation:

$$\begin{aligned} m_i(\ddot{x}_i - \ddot{x}_{i-1}) + b_i(\dot{x}_i - \dot{x}_{i-1}) + k_i(x_i - x_{i-1}) \\ = - \sum_{j=i+1}^n m_j \ddot{x}_j - m_i \ddot{x}_{i-1} \end{aligned}$$

Define $z_i = \ddot{x}_i - \ddot{x}_{i-1}$, $r_i = \sum_{j=i+1}^n \frac{m_j}{m_i} \ddot{x}_j + \ddot{x}_{i-1}$, both of which are linear combinations of accelerations. The above equation can be rewritten as

$$m_i \ddot{z}_i + b_i \dot{z}_i + k_i z_i = -m_i \ddot{r}_i \quad (6)$$

Denote $Z_i(s)$, $R_i(s)$ as the Laplace transformations of z_i and r_i , respectively. Then, Eq.(6) further gives

$$\frac{Z_i(s)}{R_i(s)} = \frac{-m_i s^2}{m_i s^2 + b_i s + k_i}$$

Let \tilde{z} and \tilde{r} be the measured values of z_i and r_i that contain noises. Using the Fourier transformations of \tilde{z}_i and \tilde{r}_i which are denoted as $\tilde{Z}_i(j\omega)$ and $\tilde{R}_i(j\omega)$, the frequency response $\frac{\tilde{Z}_i(j\omega)}{\tilde{R}_i(j\omega)}$ can be calculated. By fitting the measured frequency response with model structure shown as the right side of Eq.(7), \hat{k}_i and \hat{b}_i can be obtained.

$$\frac{\tilde{Z}_i(j\omega)}{\tilde{R}_i(j\omega)} = \frac{m_i \omega^2}{\hat{k}_i - m_i \omega^2 + \hat{b}_i \omega j} \quad (7)$$

Remark: Both methods are presented with the example of how to obtain \hat{k}_i and \hat{b}_i considering Eq.(1). Actually, the methods can be applied to all equations of Eq.(2) to obtain all structural connection parameters. Considering

the two methods, the drawback of the least-square method is easy to be discovered, that is $\tilde{\Phi}_i$ is constructed by using the integration and double integration of the measured acceleration values which are corrupted with the noises. As N becomes a large value, the accumulation effect of the noise will become significant and degrade the accuracy of the estimation results.

IV. SIMULATION ANALYSIS

In this section, the two data processing methods will be discussed further via simulation analysis.

A. Simulation setup

In the simulation, the three-rigid-body motion system is considered as an example, that is $n = 3$, where the displacement of the second rigid body can be measured in real applications using the displacement sensor such as the grating ruler or the laser interferometer. By using the feedback control, the control force can be obtained and imposed on the first rigid body with the actuator such as the linear motor or the voice coil motor. For the tracking task, the fourth-order S-curve can be adopted as the reference trajectory. The simulation setup can be seen from Fig.3, where the three accelerometers are corrupted with white Gaussian noise with the variance of 0.01m/sec^2 . The mass, stiffness and damping parameters used in the simulation are shown in Table 1. Since the parameters associated with the controller and the reference trajectory are not related with the main topic of this paper, they are omitted here. Finally, it should be noted that the sampling frequency of both the accelerometers and the controller is 5kHz .

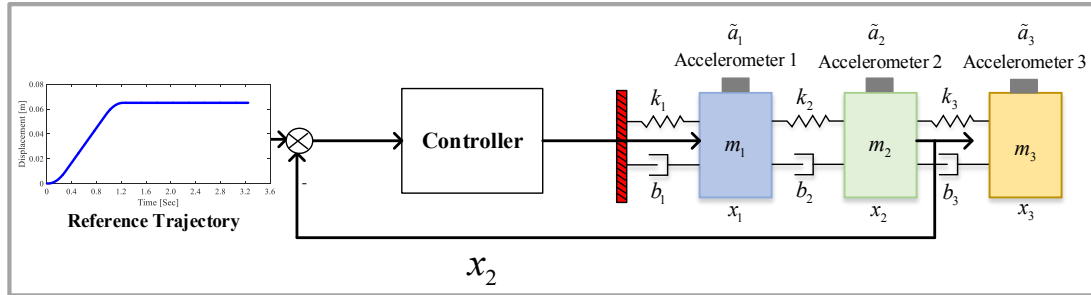


Fig.3 Schematic diagram of simulation setup.

B. Simulation results

First, the least-square method is tested, where the results can be shown in Fig.4. It can be seen that the estimated values have large uncertainties. This is primarily because that $\tilde{\Phi}_i$ is constructed by using the integration and double integration of the measured acceleration values which are corrupted with the noises. As N becomes a large value, the accumulation effect of the noise will become significant and degrade the accuracy of the estimation

results. This can be confirmed by comparing the results of $N = 500$ and $N = 100$. The estimated values for $N = 100$ has clearly lower uncertainty.

Second, the frequency-domain method is tested, where the results can be shown in Fig.5. Although the measured frequency responses $\frac{\tilde{Z}_i(j\omega)}{\tilde{R}_i(j\omega)}$ also present uncertainties, by manually fitting one frequency response with the model $\frac{m_i \omega^2}{\hat{k}_i - m_i \omega^2 + \hat{b}_i \omega j}$, it is feasible to obtain very accurate

estimated values. Of course, how to achieve high-accuracy estimated values from the measured frequency responses with the automatic software requires further investigation.

Table 1. Simulation Parameters.

	mass [kg]	stiffness [N·m]	damping [N·sec/m]
1st rigid body	$m_1 = 50$	$k_1 = 0$	$b_1 = 0$
2nd rigid body	$m_2 = 10$	$k_2 = 1.8950 \times 10^7$	$b_2 = 9.4748 \times 10^3$
3rd rigid body	$m_3 = 2$	$k_3 = 7.8957 \times 10^5$	$b_3 = 63.1655$

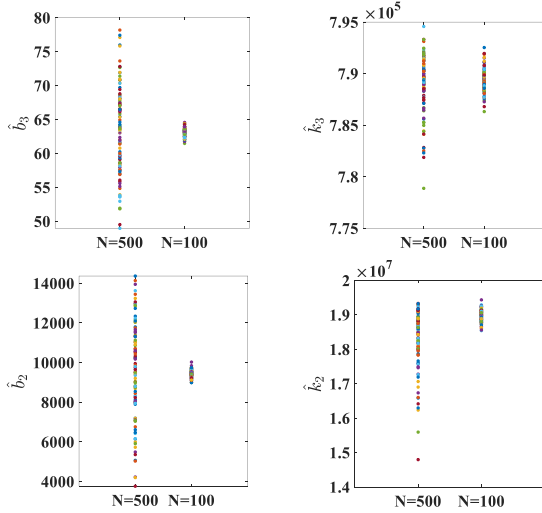


Fig.4 Parameter estimation results (100 times) with least-square method.

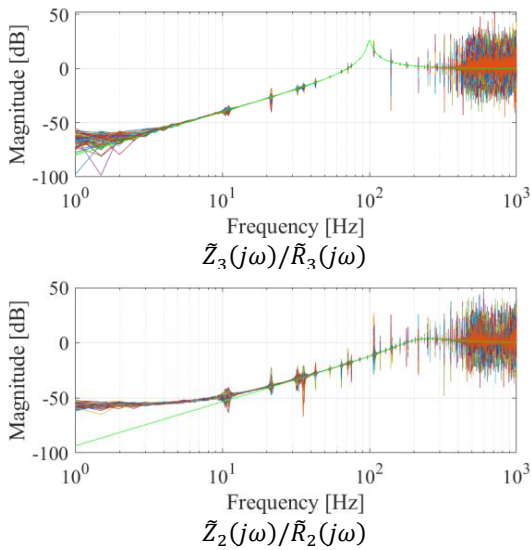


Fig.5 Measured frequency responses (100 times) compared to real frequency responses (green).

V. PRELIMINARY EXPERIMENTAL RESULTS

The 1st version of the wireless device has been developed, where the hardware components can be seen in Fig.6 and the system architecture is described as Fig.7.

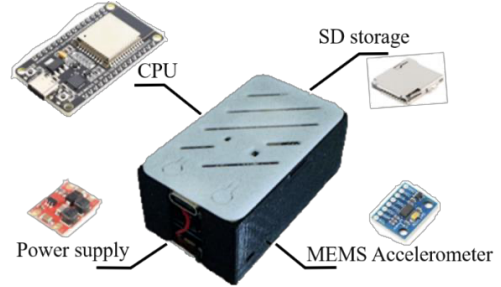


Fig.6 Hardware components of 1st version wireless device.

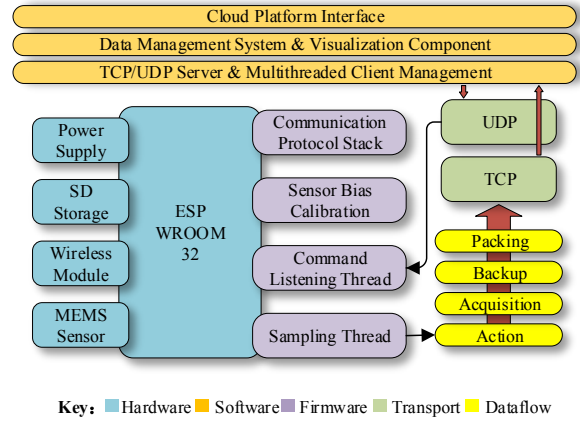


Fig.7 System architecture of 1st version wireless device.

Although there are still serious performance insufficiencies in the 1st version of the device, such as the low sampling frequency (100Hz) and the low resolution, the preliminary function testing has been conducted on a two-mass motion system shown in Fig.8. Let the 1st rigid body track a S-curve, the measurement values of the two accelerometers and the measured frequency response $\tilde{Z}_2(j\omega)/\tilde{R}_2(j\omega)$ are presented in Fig.9. The basic functional requirements have been satisfied, the development of the hardware in the following versions should consider the improvement of the sampling frequency (up to 5KHz) and the resolution.

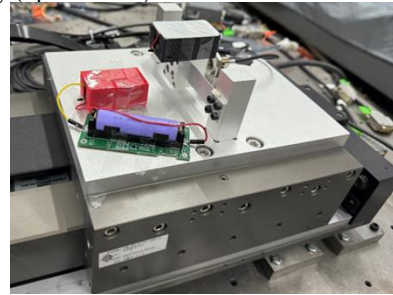


Fig.8 Preliminary function testing on a two-mass motion system.

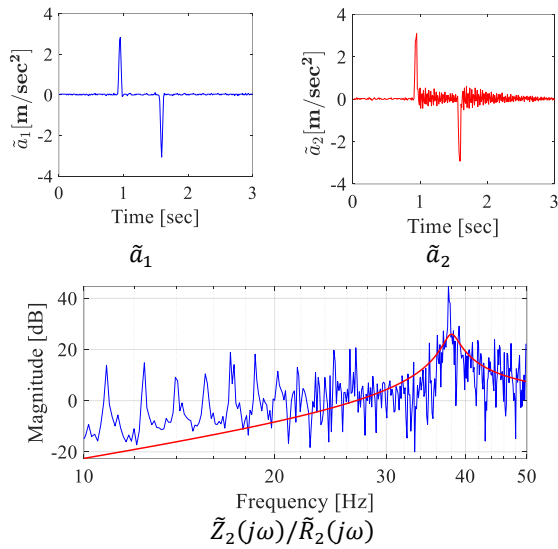


Fig.9 Preliminary experimental results

VI. CONSLUSIONS

In this paper, considering the measurement problem for the structural connection parameters of the multi-rigid-body motion system, this paper proposes a measurement scheme using multiple wireless accelerometers and discusses the candidate data processing methods. As a conclusion, the frequency-domain identification method is more preferable than the least-square method for real applications with sensor noises, since the integration of the measurement values of the accelerometers required in the least-square method causes the significant noise accumulation effect.

Through the verification on the first-version device developed recently, it has been identified that the sampling frequency and the resolution are two major factors for the single device. In addition, the lightweight design of the device and the calibration of the used accelerometers should further be considered [9]. For networked measurement for the structural connection parameters, the time synchronization of data is also crucial, which should be seriously considered in the future [10]. Finally, the uncertainty evaluation method of the frequency-domain identification method should also be studied by referencing the existing beneficial results [11-12].

REFERENCES

[1] T.Oomen, “Advanced motion control for next-generation precision mechatronics: Challenges for control, identification, and learning”, Proc. of 3rd

IEEJ International Workshop on Sensing, Actuation, Motion Control, and Optimization, 2017, pp.1-12.

[2] M.F.Heertjes, H.Butler, N.J.Dirx, S.H.van der Meulen, et al., “Control of wafer scanners: Methods and developments”, Proc. of 2020 American Control Conference, 2020, pp.3686-3703.

[3] K.Classesens, W.M.Heemels, T.Oomen, “Digital twins in mechatronics: From model-based control to predictive maintenance”, Proc. of 2021 IEEE 1st International Conference on Digital Twins and Parallel Intelligence, 2021, pp.336-339

[4] K.Classesens, M.Mostard, J.Van De Wijdeven, W.M.Heemels, et al., “Fault detection for precision mechatronics: Online estimation of mechanical resonances”, IFAC-PapersOnLine, vol.55, No.37, 2022, pp.746-751.

[5] N.Wengert, M.Nefzi, P.Eberhard, B.Geuppert, “Dynamics in lithographic projection objectives”, Multibody Syst. Dyn., vol.30, February 2013, pp. 233-245.

[6] Y.M.Al-Rawashdeh, M.Al Janaideh, M.Heertjes, “On characterization of a generic lithography machine in a multi-directional space”, Mech. Mach. Theory, vol.170, April 2022, pp.104638.

[7] Y. M. Al-Rawashdeh, M. Al Janaideh, M. F. Heertjes, “A suppress-excite approach for online trajectory generation of uncertain motion systems”, Mech. Syst. Signal Pr., vol. 186, March 2023, pp. 109769.

[8] G.Maculotti, M.Marschall, G.Kok, B.A.Chekh, et al., “A Shared Metrological Framework for Trustworthy Virtual Experiments and Digital Twins”, Metrology, vol.4, No.3, July 2024, pp.337-363.

[9] T.Bruns, H.Volker, S.Eichstädt, “Using opensource software tools for data analysis in high intensity shock calibration of accelerometers”, Proc. of IMEKO 23rd TC3, 13th TC5 and 4th TC22 International Conference, 2017.

[10] S.Eichstädt, A.P.Vedurmudi, M.Gruber, D.Hutzschenreuter, “Fundamental aspects in sensor network metrology”, Acta IMEKO, vol.12, No.1, March 2023, pp.1-6.

[11] S.Eichstädt, C.Elster, I.M.Smith, T.J.Esward, “Evaluation of dynamic measurement uncertainty—an open-source software package to bridge theory and practice”, J. Sens. Sens. Syst., vol.6, No.1, February 2017, pp.97-105.

[12] T.Esward, S.Eichstädt, I.Smith, T.Bruns, et al., “Estimating dynamic mechanical quantities and their associated uncertainties: application guidance”, Metrologia, vol.56, No.1, November 2018, pp.015002.